View metadata, citation and similar papers at core.ac.uk
brought to you by CORE
provided by Springer - Publisher Connector

Journal of ELECTRONIC MATERIALS, Vol. 36, No. 10, 2007
DOI: 10.1007/s11664-007-0206-5
© 2007 TMS

Regular Issue Paper

Current-Induced Phase Partitioning in Eutectic Indium-Tin Pb-Free Solder Interconnect

JOHN P. DAGHFAL[1] and J. K. SHANG[1,2,3]

1.—Shenyang National Laboratory for Materials Science, Institute of Metals Research, CAS, Shenyang 110016, China. 2.—Department of Materials Science and Engineering, University of Illinois at Urbana-Champaign, Urbana IL61801, USA. 3.—e-mail: jkshang@uiuc.edu

Structural changes from high-density electric currents were examined in a eutectic In-Sn/Cu interconnect. Under electrical loading, Sn and In migrated in opposite directions, creating a partition of the Sn- and In-rich phases between the anode and the cathode. At the anode, a net gain of Sn atoms resulted in the formation of massive, columnar hillocks on the surface, but a net loss of In led to dissolution and disappearance of the In-rich intermetallic layer. At the cathode, the exodus of Sn left valleys adjacent to the In-rich regions on the surface, while the amount of the In-rich phase grew, due to the net influx of In at the expense of the In-rich intermetallic layer.

Key words: In-Sn solder, electromigration, current stressing, hillocks, interface

INTRODUCTION

US and European directives banning lead (Pb) have served as an impetus to drive research on Pb-free solders. While much of the attention has been focused on leading replacement candidates (such as Sn-Ag-Cu) for the eutectic Pb-Sn solder, industries also need to find unique Pb-free solutions to fit specific applications. In optoelectronic and photonic devices, the polymeric coatings of the optical fibers and ribbons have a low glass transition temperature, T_g. Thus, they are very sensitive to high production temperatures, so solders of high melting temperatures should be avoided. In addition, to achieve the strict optical alignment in those devices, solder connections must accommodate large displacements without incurring large stresses. Indium-tin solders meet these special needs in optoelectronics and photonics applications because of their low melting temperatures, deformability, and chemical compatibility.

The microstructures of In-Sn alloys have been well documented. The binary phase diagram for indium-tin alloy shows a low melting eutectic at intermediate compositions. The eutectic is formed between phases of intermediate composition, unlike the Sn-Pb systems where the phases are terminal solid solutions. The compositions are highly disordered at ordinary temperatures, and their broad solubility ranges and mechanical properties resemble the behavior of solid solutions rather than the behavior ordinarily found in intermetallic compounds.[1] The phase diagram also indicates that In solubility in Sn is nearly constant at temperatures between the melting point (120°C) and 20°C, while Sn solubility in In decreases from 44.8 wt.% at 120°C to about 28 wt.% at 20°C. The microstructure of eutectic indium-tin solder alloy is predominantly composed of two intermetallic phases, an In-rich β phase and a Sn-rich γ phase. In reflow soldering, the phase compositions are dependent on the cooling rates of the solder joint after reflow.[2] Mei and Morris describe the microstructure as a light colored, Sn-rich, polygranular area consisting of equiaxed grains interspersed with dark colored In-rich particles.[3] For eutectic In-Sn solder on a Cu substrate, it has been reported that the β phase, which is pseudo-BCC tetragonal in structure, is 44.8 wt.% tin, while the γ phase, which is hexagonal in structure, is 77.6 wt.% Sn.[4,5] The Metals handbook shows the microstructure of as-reflowed In-Sn eutectic solder as having homogeneous and uniformly dispersed In-rich grains throughout the joint.[6] The In-rich phase is very soft, while the

(Received January 20, 2007; accepted May 8, 2007; published online August 22, 2007)

Sn-rich phase is relatively hard.[4] Previous work has indicated that the high solubility of Cu in the Sn-In solder system defines the formation of the intermetallic compound (IMC) layers of $Cu_2(Sn, In)$ and Cu_2In_3Sn at the copper/solder interface, with the Cu_2In_3Sn on the solder side of the interface.[2]

The creep behavior of In-Sn eutectic solder has also been studied.[4] Additional studies have been published on the microstructure, intermetallic compounds and reliability of eutectic In-Sn on Ni and Au substrates.[4,7] However, there is little known about the electrical behavior and properties of this solder alloy. Reliability studies on indium solders used in semiconductor lasers were recently reported by Liu *et al.*[8] Catastrophic degradation was observed in the solder joints after exposure to 6 A current at 35°C for 500 h. The failure was sudden, suggesting a short degradation time period. The observation of voids, blisters and indium accumulation spots led to the conclusion that electromigration had caused the failure in the system.

The purpose of this investigation was to determine the microstructural response of the eutectic indium-tin solder interconnect system to electric loading. For this purpose, microjoints of the eutectic In-Sn solder with Cu were made by reflow soldering. The solder interconnects were then exposed to high-density electric currents for various lengths of time. Current stressing caused drastic changes in both the solder microstructure and the interfacial intermetallic compounds. Massive Sn-rich hillocks were found near the anode and Sn-depletion regions near the cathode. As a result of electromigration, the Cu-Sn intermetallic layer grew in thickness, while the In-rich intermetallic layer was dissolved.

EXPERIMENTAL

The eutectic indium-tin solder paste, composed of In-48Sn, was provided by the Indium Corporation of America (NY, USA). The solder interconnect specimens were prepared by the reflow soldering of two Cu (>99.99% purity) substrates together in a fashion similar to that previously published by Yang and Shang.[9] After the surfaces of the copper cubes had been polished, they were cut down to a cross-section of about 400 μm × 400 μm by electric discharge machining. The two bars were aligned and clamped at a distance of about 100 μm apart. The solder was placed between the bars and reflowed at a temperature of 140°C, then it was cooled to room temperature. After reflow, the bar samples were mounted in a sample holder using extremely strong rapid cure adhesive. A series of grinding and polishing steps followed to flatten each side of the bars.

The setup for the current stressing experiment is shown in Fig. 1. The interconnect sample was mounted on a glass slide with both ends covered with a small, thin, copper sheet around 100 μm in thickness. The Cu sheets and the sample were then firmly clamped together with the glass slide. The copper sheets were connected to a constant current source via copper leads. The entire sample fixture was immersed in a heat-conductive oil bath to minimize temperature gradient and temperature rise, as both are known to induce thermomigration in solder joints.[10]

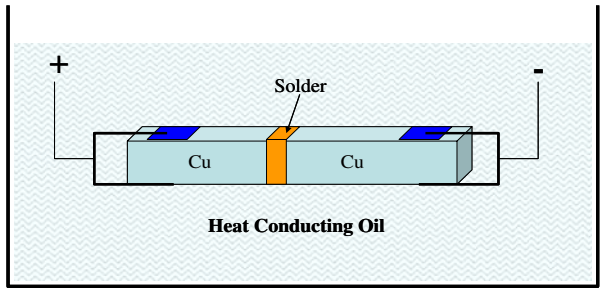

Fig. 1. Current stressing experimental setup.

The current density at which the solder joint becomes liquid is taken as the critical current density. Using a high magnification microscope, we tested multiple samples, and the average critical current density was determined to be 2.8×10^4 A/cm^2. The current density was set at 2.6×10^4 A/cm^2 and the exposure time at 72 h for this study. The time duration and current were monitored with a digital multimeter. The sample temperature was regularly checked with a thermocouple. The sample temperature during the current stressing experiment varied but did not exceed 80°C. After current stressing, the samples were carefully removed from the fixture and cleaned with a hexane solution for further observations.

For microscopic observations, the samples were mounted and ground with SiC grinding paper, with a grit of 2000. The final specimen cross-section size after grinding was around 200 μm × 200 μm. A grind–polish–etch method was used to prepare the desired face and to remove any contamination, such as SiC grains. The final step was necessary, since the solder was relatively soft and easily contaminated. A JEOL field-emission scanning electron microscope (SEM), equipped with an Oxford energy dispersive spectroscopy (EDS) system, was then used to analyze the samples. Both line scans and single point analysis were conducted to study microstructure changes across the solder joint.

RESULTS

Initial Microstructure

The SEM images of the solder microstructure of the as-reflowed sample are shown in Fig. 2 as a mixture of light colored background interspersed intermittently with dark colored regions. EDS showed that the dark regions are In-rich (β phase), with 66.9 wt.% In, and the light colored regions are Sn-rich (γ phase), with 77.2 wt.% Sn. The as-reflowed microstructure is, therefore, a mixture of γ

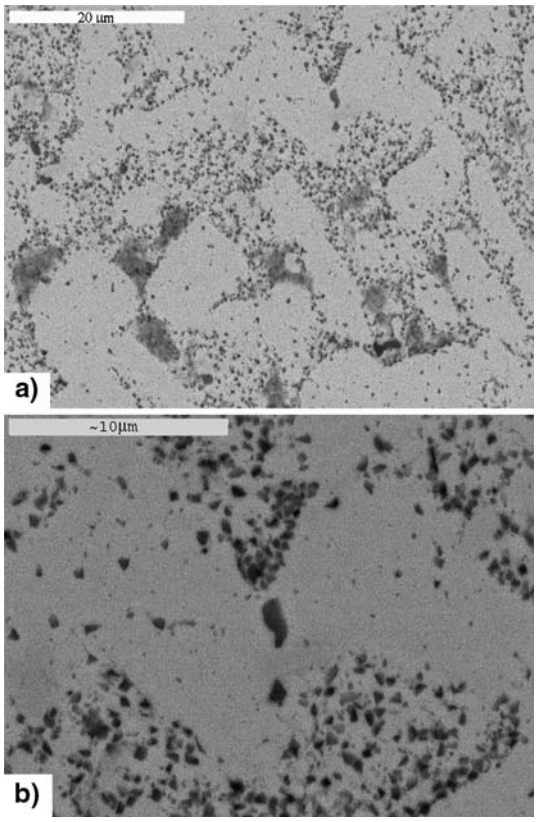

Fig. 2. (a) SEM image of the microstructure of eutectic In-Sn solder after reflow (before current stressing); (b) light areas are Sn-rich γ phase, with 77.2 wt.%, and the dark areas are In-rich, β phase, with 66.9 wt.%.

dendrites and $\alpha + \beta$ eutectic. The appearance of the γ dendrite is apparently a result of the fast cooling, which is known to promote dendritic structure in other eutectic Pb-free solder systems (Sn-Ag and Sn-Ag-Cu).[11]

Intermetallic Compounds

The intermetallic structure produced at the eutectic In-Sn interface with Cu is shown in Fig. 3, where two distinct layers of intermetallic compounds were formed after reflow. Similar to the intermetallic structure formed with Sn-Bi or Sn-Pb, the interfacial reaction created a double layer made of two intermetallic phases. Unlike Sn-Bi and Sn-Pb solders, where Sn is the only active element with the Cu substrate, both In and Sn participated in the interfacial reaction with Cu. EDS showed that the primary IMC, immediate to Cu, was Cu-rich, containing 24.4 wt.% In, 27.9 wt.% Sn and 47.7 wt.% Cu, while the secondary IMC, next to the solder, was In-rich, with the following element concentrations: In 51.8 wt.%, Sn 20.0 wt.%, Cu 28.2 wt.%. The average primary IMC thickness before current stressing was 1.1 μm, and the secondary IMC layer was slightly thicker. These results agree with earlier published findings.[4,5]

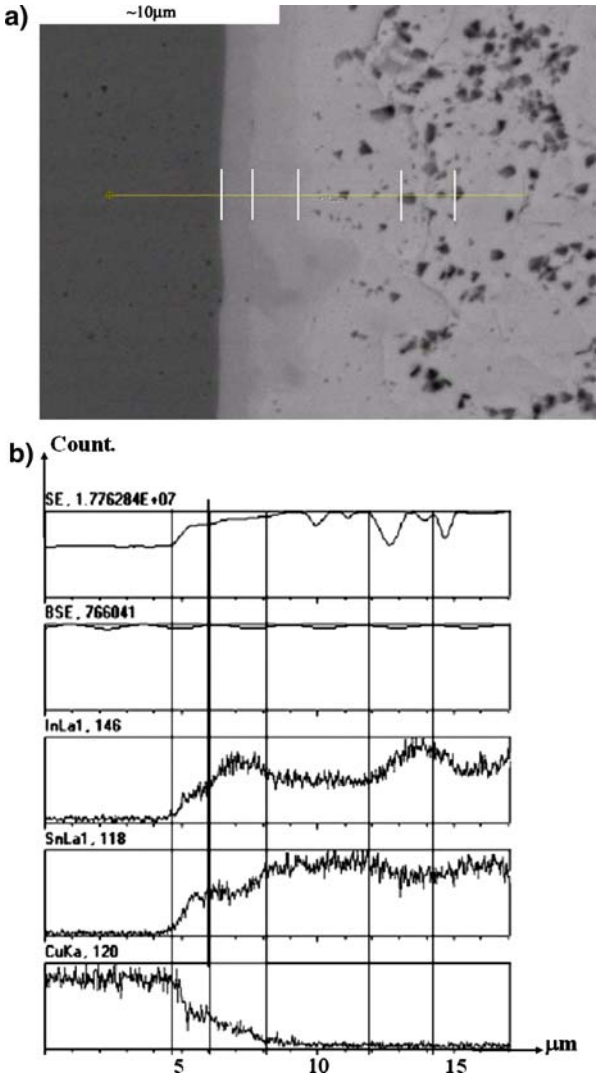

Fig. 3. Intermetallic compound (IMC) morphology. The interface between Cu and In-Sn solder shows a double IMC (a) Cu-rich primary and In-rich secondary (near the solder side). The EDS line-scan results corresponding with the SEM image in (a) is shown in (b).

Current-Induced Microstructural Changes

At a low current density of 2.0×10^4 A/cm^2 for an exposure time of 72 h, some surface deposits (hillocks) were found in the solder near the anode, but the features were not clearly defined. At an increased density of 2.6×10^4 A/cm^2, Fig. 4 showed that severe hillock formation occurred at the anode side. As discussed above, before current stressing, the microstructure was a mixture of Sn dendrites and In-rich regions (Fig. 4a). After current stressing, massive hillocks were formed near the anode (Fig. 4b). Near the cathode, the surface became rougher as depressions and valleys were created, apparently by evacuation of the solid matter. Therefore, the electric current caused a net gain of matter near the anode but a net loss at the cathode.

The detailed structure of hillocks and valleys are presented in Fig. 5. The hillocks assumed a columnar

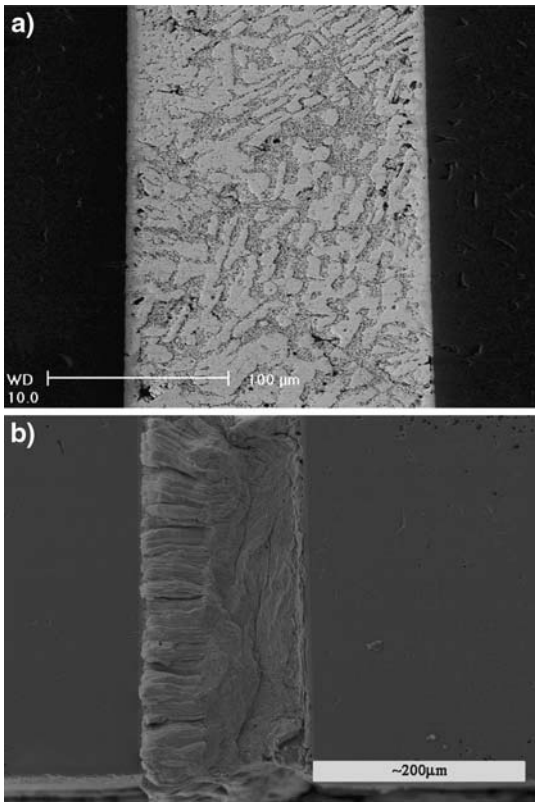

Fig. 4. SEM image of the eutectic In-Sn solder joint before current stressing (a), and SEM image of the same sample after current stressing (b). Left side is the anode side. Current flowing from left to right.

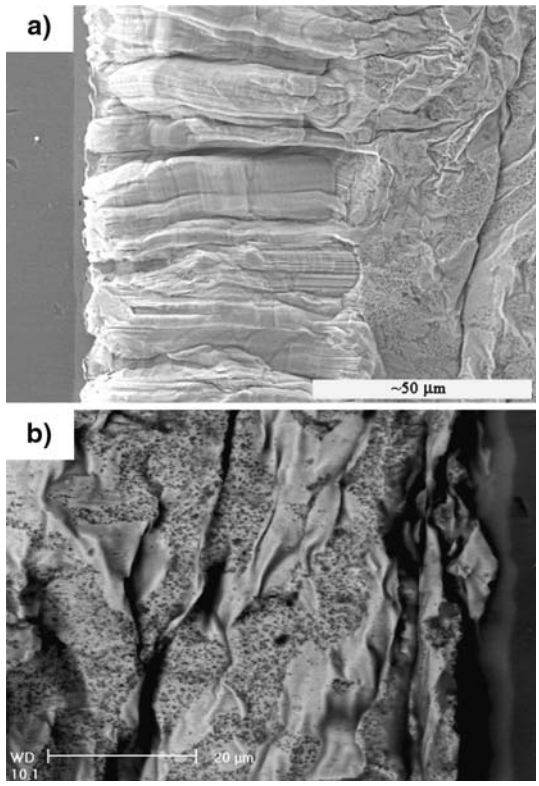

Fig. 5. SEM images of the eutectic In-Sn solder after current stressing. (a) Hillocks at the anode and (b) In-rich phase near the cathode.

structure roughly parallel to the current direction (Fig. 5a). Each column, outlined by striations, extended nearly halfway through the solder section. Compositional analysis indicated that the region with hillocks was Sn rich, containing 75 wt.% Sn. The hillocks themselves were nearly pure Sn. On the cathode side, formation of the depressions and valleys on the sample surface exposed slopes and plateaus densely populated with the In-rich phase (Fig. 5b). The In concentration was increased to 72 wt.%. The enrichment of Sn at the anode and In at the cathode points to the electromigration of Sn and In along opposite directions. As a result of the electromigration, the alloy constituents were separated in the solder interconnect, with the Sn-rich phase concentrated at the anode and the In-rich phase accumulating near the cathode.

The constituent partitioning is not just confined to the surface layer. About 100 μm from the surface, Fig. 6 showed segregations of Sn and In similar to those at the anode and cathode side, respectively. On the anode side, there is a γ-Sn-rich zone that corresponds to the hillock formation on the surface. On the cathode side of the solder joint, as is evident in Fig. 6b, there is an apparent increase in the β-phase particles, as larger dendrite-like formations of In particles are present near the primary IMC on the cathode side. In-rich particles accumulated on the edge of the Sn-rich hillock region, forming an In-rich 'diffusion' line (see arrow in Fig. 6a).

The evolution of the interfacial intermetallic compounds is also evident in Fig. 6. At the anode, the primary Cu-rich IMC layer almost doubled in thickness and increased in Cu concentration by 10 wt.%, while the In-rich secondary IMC layer disappeared as it was overtaken by the Sn-rich hillocks. On the cathode side, the Cu-rich primary IMC layer tripled in thickness and had a 10 wt.% increase in Cu concentration, while decreasing in In concentration by 6 wt.%. The secondary IMC layer was dissolved into the solder, further increasing the In concentration near the cathode.

DISCUSSION

The results of this study have shown that In and Sn responded differently to high-density electric currents. Under the electric current, Sn migrates to the anode but In to the cathode. These migration directions are contrary to those in the Sn-Bi system, where Bi is forced to the anode and Sn to the cathode.[9]

In pure metals, the driving force for electromigration, F_{em}, may be written as[12]

$$F_{\mathrm{em}} = Z^{*} e \rho J \qquad (1)$$

where Z^{*} is the effective charge of the species, e, electron charge, ρ, the electrical resistivity, and J,

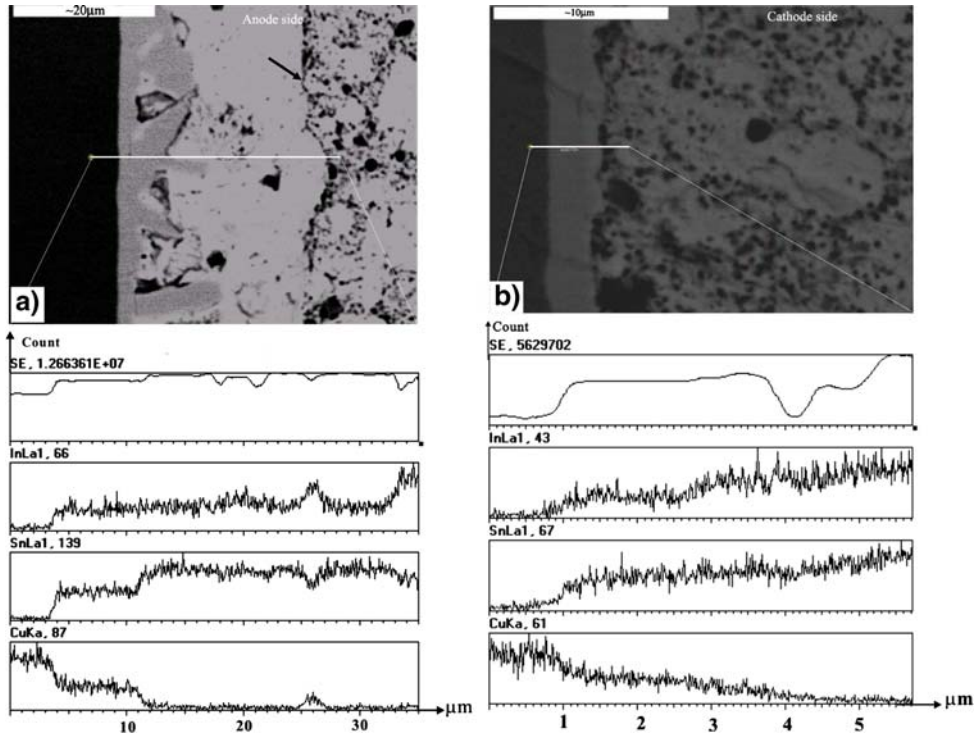

Fig. 6. SEM images and their corresponding EDS line scans of the In-Sn solder joint after grinding down to the middle of the sample. (a) At the anode side, (b) at the cathode side.

the current density. The effective charge of Sn and In is –18 and –2, respectively.[13] Because their ions are negative, both Sn and In are expected to migrate along the same direction as electrons, namely from the cathode to the anode, according to Eq. 1. While Eq. 1 agrees with the migration of Sn in this study, it appears to conflict with the observation that In has moved and accumulated near the cathode.

In binary alloys, where both components want to migrate in the same direction, only one species can migrate in this preferred direction, while the other is displaced in the opposite direction. Which component emerges as the "prime mover" is determined by the relative magnitude of the electromigration driving force[14] and the relative diffusivity. At room temperature, the diffusivities of Sn and In in Sn-In alloy are not much different: $2.29–2.47 \times 10^{-18}$ cm^2 s^{-1} for In and 2.62×10^{-18} cm^2 s^{-1} for Sn.[15] On the other hand, the driving force for Sn migration to the anode is much greater because of its higher effective charge and electrical resistivity. Therefore, Sn would act as the "prime mover" along the preferred direction.

As the two components were separated to the two electrodes, both the composition and the stability of the IMCs were affected. It was previously thought that, due to the polarity effect, the electrons flow from the IMC to the solder at the cathode side, while, at the anode, the flow direction is reversed. In the Sn-Cu couple, electromigration would enhance IMC formation at the anode but promote IMC dissolution at the cathode.[16] In this research, however, the IMC dissolution in the primary Cu-rich IMC did not occur at the anode or cathode sides, while the secondary In-rich IMC adjacent to the solder was almost completely dissolved. At the same time, both primary IMCs increased in size and Cu concentration, indicating that, even during current stressing, thermally activated reactions between the solder and the Cu substrate continued to take place.

CONCLUSIONS

Under high current density, electromigration occurred in which the Sn and In were driven towards the anode and cathode ends of the solder joints, respectively. Such observations agree with the notion that, in binary alloys, the alloying component with the greater electromigration driving force takes the preferred direction of migration, while the other component is displaced along the opposite direction. The build-up of Sn at the anode resulted in the formation of a region of Sn-rich columnar hillocks. As In was displaced to the cathode and the In-rich IMCs were dissolved by electric current, the volume fraction of the β phase was increased, adjacent to the cathode IMC.

ACKNOWLEDGEMENTS

Support for this study was provided by the Chinese Natural Sciences Foundation, grant #

50228101, and the National Basic Research Program of China, grant # 2004CB619306. The authors also owe special thanks to Dr. Warke, Q.L. Yang and others in the Microelectronics Laboratory at IMR for their assistance.

REFERENCES

1. R. Kubiak, M. Wolcyrz, and W. Zacharko, *J. Less-Common Met.* 65, 263 (1979).
2. J.W. Morris, J.L. Goldstein Freer, and Z. Mei, *JOM* 45, 25 (1993).
3. Z. Mei and J.W. Morris Jr., *J. Electron. Mater.* 21, 401 (1992).
4. J.L. Freer and J.W. Morris Jr., *J. Electron. Mater.* 21, 647 (1992).
5. M. Abtew and G. Selvaduray, *Mater. Sci. Eng.* 27, 95 (2000).
6. C.J. Thwaites, *Atlas of Microstructures of Industrial Alloys*, in *The Metals Handbook*, ed. R.F. Mehl (The American Society for Metals: Metals Park, 1972), pp. 317–320.
7. S.S. Wang, Y.H. Tseng, and T.H. Chuang, *J. Electron. Mater.* 35, 165 (2006).
8. X. Liu, R.W. Davis, L.C. Hughes, M.H. Rasmussen, R. Mhat, and C.-E. Zah, *J. Appl. Phys.* 100, 1 (2006).
9. Q.L. Yang and J.K. Shang, *J. Electron. Mater.* 34, 1363 (2005).
10. H. Ye, C. Basaran, and D.C. Hopkins, *Appl. Phys. Lett.* 82, 1045 (2003).
11. J. Sigelko, S. Choi, K.N. Subramanian, J.P. Lucas, and T.R. Bieler, *J. Electron. Mater.* 28, 1184 (1999).
12. H.B. Huntington and A.R. Grone, *J. Phys. Chem. Solids* 20, 76 (1961).
13. K.V. Reddy and J.J.B. Prasad, *J. Appl. Phys.* 55, 1546 (1984).
14. S.G. Epstein, *Liquid Metals: Chemistry and Physics*, ed. Beer S.Z. (Marcel Dekker, New York, 1972), pp. 537–584.
15. M. Komiyama, H. Tsukamoto, T. Matsuda, and Y. Ogino, *J. Mater. Sci. Lett.* 5, 673 (1986).
16. K.N. Tu, *J. Appl. Phys.* 94, 5451 (2003).